ELSEVIER

International Journal of Mass Spectrometry 204 (2001) 125–131

International Journal of Mass Spectrometry

Complexes of Li atoms with water and ammonia: a combined neutralization–reionization mass spectrometry and theoretical study

Jianglin Wu, Michael J. Polce, Chrys Wesdemiotis*

Department of Chemistry, The University of Akron, Akron, OH 44325, USA

Received 9 March 2000; accepted 10 April 2000

Abstract

The hypervalent complexes of Li atom with water and ammonia, viz. Li–OH_2 and Li–NH_3, are generated in the gas phase by neutralization of Li^+–OH_2 and Li^+–NH_3, respectively. The mass spectra obtained by subsequent reionization ~0.3 μs later clearly indicate that the neutral complexes Li–OH_2 and Li–NH_3 are stable species in the gas phase, as had been predicted by theory. Li–OH_2/Li–NH_3 dissociate partly to Li+H_2O/NH_3 within the timescale of the experiments, the dissociating fraction of the water complex being larger. Parallel ab initio calculations reveal that the more extensive dissociation of Li–OH_2 versus Li–NH_3 is the result of a lower binding energy (51 versus 62 kJ mol^{-1} for Li–OH_2 and Li–NH_3, respectively) and a less favorable Franck-Condon factor for transitions between Li–OH_2 and Li^+–OH_2, as compared to transitions between Li–NH_3 and Li^+–NH_3. (Int J Mass Spectrom 204 (2001) 125–131) © 2001 Elsevier Science B.V.

Keywords: Hypervalent species; Li-atom complexes; Solvated Li atom; Neutralization–reionization

1. Introduction

The complexes between alkali metal atoms and Lewis base molecules may be viewed as charge transfer complexes because the electron lone pair of the base can be delocalized into vacant metal atom orbitals [1]. According to theory, there is considerable bonding between the metal atom and the base, which is further enhanced by electron correlation effects, charge polarization of the metal atom, and electrostatic interactions within the complex [2–12]. A large number of computational studies has so far interrogated the structures and stabilities of alkali atom–Lewis base complexes [1–14]; this interest has been spurred by the implication that such complexes, which are nominally hypervalent [10], are (1) intermediates in reactions involving alkali metal atoms [13], (2) limiting models for excess electrons in metal–solvent systems [2], and (3) test cases for electrostatic models of bonding [14].

Li–OH_2 and Li–NH_3 are prototype metal atom–Lewis base complexes. An early ab initio molecular orbital study by Nicely and Dye predicted a binding energy of ~84 kJ mol^{-1} for Li–NH_3 [2]. Later calculations by Trenary et al. on a family of alkali atom–Lewis base complexes found that Li binds stronger to NH_3 than to H_2O, the corresponding bond

* Corresponding author. E-mail: wesdemiotis@uakron.edu

PII S1387-3806(00)00333-X

energies being 61 and 54 kJ mol^{-1}, respectively [1]. A reinvestigation of Li–OH_2 by Curtiss and Pople revealed that the electron correlation contribution to the bond energy is 13 kJ mol^{-1} and that the optimized geometry of $LiOH_2$ is nonplanar, with Li bent off the OH_2 plane by 40.1° at the MP4/6-311G** level [8]. A comparison of the calculated vibrational frequencies of Li–OH_2 and Li–NH_3 further indicated that Li can bend off its equilibrium angles (wag) much more easily in the H_2O than in the NH_3 complex [5].

$LiOH_2$ and $LiNH_3$ have been detected experimentally in frozen argon matrices by infrared and electron spin resonance spectroscopy [15–17]. These complexes, as well as analogous Na and K compounds, have also been formed in molecular beams for measurement of their vertical ionization energies by photoionization mass spectrometry [18–23]. Other chemical or physical properties of Li–OH_2 and Li–NH_3 have not been determined experimentally. The present study obtains new insight about the intrinsic chemistry of $LiOH_2$ and $LiNH_3$ by means of neutralization–reionization mass spectrometry (NRMS) [24–26]. The complexes are generated in the gas phase by reduction of the corresponding cations and characterized by the mass spectra arising after reoxidation [27–30]. In addition, ab initio molecular orbital (MO) theory is employed to elucidate the redox behavior and relevant thermochemistry of the couples $LiOH_2$/Li^+OH_2 and $LiNH_3$/Li^+NH_3.

2. Methods

All experiments were performed on a modified Micromass AutoSpec tandem mass spectrometer of E_1BE_2 geometry [31], which contains two collision cells, separated by an intermediate ion deflector, in the field-free region between the magnet (B) and the second electric sector (E_2). This configuration permits the acquisition of various types of tandem mass spectra, including collision-activated dissociation (CAD) and neutralization–reionization (NR) spectra. The instrument and the detailed acquisition protocol for CAD and NR mass spectra have been reported elsewhere [29,31].

The precursor ions $LiOH_2^+$ and $LiNH_3^+$ were formed by fast atom bombardment (FAB) ionization, using a 20 keV cesium ion gun as the source of primary particles. The sample used to produce $LiOH_2^+$ was a solution of a few milligrams lithium trifluoroacetate in 1–2 mL concentrated sulfuric acid. A few milligrams ammonium sulfate were added to this solution to produce $LiNH_3^+$. Approximately 1–2 μL of the final solutions were introduced into the FAB source. The secondary ions generated by FAB were accelerated to 8 keV upon leaving the ion source. The ^{7}Li isotopomers of $LiOH_2^+$ (*m/z* 25) and $LiNH_3^+$ (*m/z* 24) were mass-selected by E_1B for the measurement of CAD and NR spectra; the product ions arising from these processes were mass analyzed by scanning E_2. Trimethylamine (TMA) served as the neutralization target and O_2 as the reionization or CAD target. The pressure of each collision gas was gradually increased until the intensity of the mass-selected precursor ion was attenuated by ~25%. The CAD spectra shown combine 50 added scans, whereas the shown NR spectra of $LiNH_3^+$ and $LiOH_2^+$ are the sums of ~4000 and 2000 scans, respectively. All chemicals were purchased from Aldrich and were used as received.

The structures and energetics of $LiOH_2$ and $LiNH_3$ and of the corresponding cations were evaluated by parallel ab initio MO calculations, run on a pentium PC using GAUSSIAN 94 for Windows [32] interfaced with CHEM-3D [33]. Geometry optimization and energy minimization were computed at the MP2/6-311++G(*d,p*) level of theory.

3. Results and discussion

3.1. Precursor ions Li^+OH_2 and Li^+NH_3

The CAD spectra of Li^+OH_2 (*m/z* 25) and Li^+NH_3 (*m/z* 24) are shown in Figs. 1 and 2, respectively (^{7}Li isotopomers unless specified otherwise). CAD of Li^+OH_2 leads to $LiOH_{0-1}^+$ (*m/z* 23–24), $H_{0-2}O^+$ (*m/z* 16–18), and Li^+ (*m/z* 7); such products agree well with the connectivity Li^+–OH_2. CAD of Li^+NH_3 gives rise to the fragments $LiNH_{0-2}^+$ (*m/z* 21–23), NH_{0-3}^+ (*m/z* 14–17), and Li^+ (*m/z* 7) which, again,

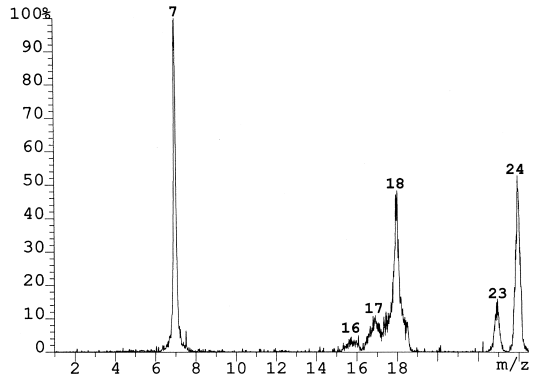

Fig. 1. CAD mass spectrum of Li^+OH_2 (*m/z* 25). A composite signal is observed for *m/z* 18 ($H_2O^{+\cdot}$). The peak widths of the narrow and broad components are 65 V (at half-height) and 410 V (across the dish), respectively.

support the connectivity Li^+–NH_3. The CAD spectrum of Li^+NH_3 also displays small peaks at *m/z* 18 ($H_2O^{+\cdot}$) and 6 ($^6Li^+$), indicating that the Li^+NH_3 beam is contaminated by a small amount of isobaric $^6Li^+OH_2$ (both of *m/z* 24). Based on the abundance ratio (*m/z* 18):(*m/z* 7) in Figs. 2 and 1, the proportion of $^6Li^+OH_2$ in the Li^+NH_3 beam is ~2%.

It is noticed that the CAD signals for $H_2O^{+\cdot}$ (*m/z* 18) and $NH_3^{+\cdot}$ (*m/z* 17) are composite, with narrow, Gaussian components superimposed onto broad, dish-topped components (Figs. 1 and 2). The central, narrow peaks are ascribed to the direct dissociations

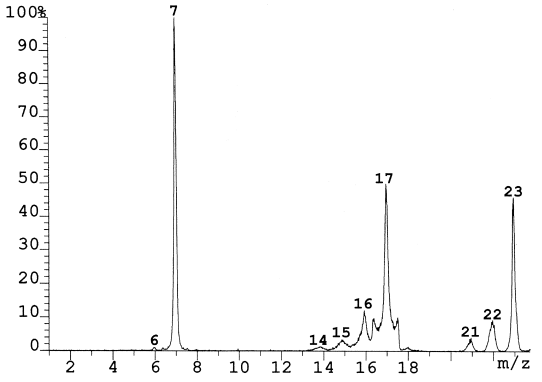

Fig. 2. CAD mass spectrum of Li^+NH_3 (*m/z* 24). A composite signal is observed for *m/z* 17 ($NH_3^{+\cdot}$). The peak widths of the narrow and broad components are 61 V (at half-height) and 440 V (across the dish), respectively.

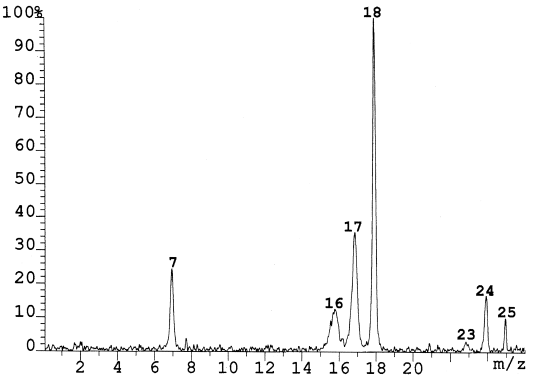

Fig. 3. NR mass spectrum of Li^+OH_2 (*m/z* 25).

Li^+OH_2 (Li^+NH_3) → $OH_2^{+\cdot}$ ($NH_3^{+\cdot}$). On the other hand, the broad peaks are attributed to fragmentation after charge stripping [34], as illustrated in

$$Li^+–OH_2 \text{ (CAD with } O_2) \rightarrow [Li^+ \cdots OH_2^{+\cdot}]^* \rightarrow Li^+ + H_2O^{+\cdot} \quad (1)$$

for the H_2O complex. The $LiOH_2^{2+\cdot}$ ($LiNH_3^{2+\cdot}$) dications generated upon charge stripping most likely lie on a dissociative surface and, thus, decompose with a significant reverse activation energy which in turn causes the broad, dish-topped shapes observed. The Li^+ fragments co-generated in this process should also yield broad peaks. Indeed, the base of *m/z* 7 (Figs. 1 and 2) appears to contain a broad component; its smaller relative abundance vis à vis the broad $H_2O^{+\cdot}/NH_3^{+\cdot}$ signals must be due to the more severe scattering losses and poorer transmission efficiency of the lighter Li^+ fragment [34]. The wide $H_2O^{+\cdot}/NH_3^{+\cdot}$ peak components disappear when the CAD target is changed from O_2 to He, in keeping with the markedly lower charge-stripping cross section of the latter target gas [34].

3.2. Generation and characterization of gaseous $LiOH_2$ and $LiNH_3$

Neutralization of $LiOH_2^+$ (*m/z* 25) with trimethylamine and subsequent reionization of the intermediate neutral(s) with oxygen leads to the NR spectrum of Fig. 3. The recovered Li^+OH_2 ion (*m/z* 25) in this

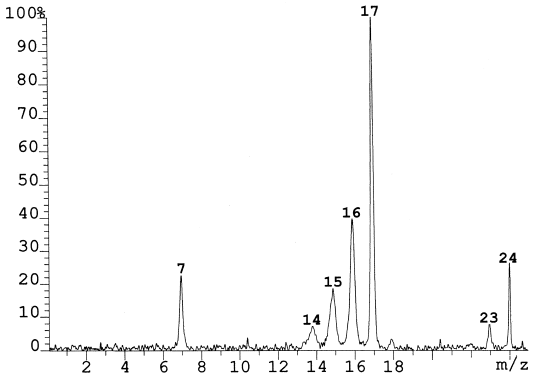

Fig. 4. NR mass spectrum of Li^+NH_3 (*m/z* 24).

spectrum indicates that the intermediate neutral $LiOH_2$ has survived intact between the neutralization and reionization events (average lifetime ~0.3 μs [31]). For this, $LiOH_2$ must be a bound species with a considerable dissociation energy. This result unequivocally shows that the $LiOH_2$ complex is stable in the diluted gas phase, as predicted by theory [1,2,5,35].

The NR spectrum of Li^+OH_2 contains all fragments present in the CAD spectrum. The only significant difference is the higher relative intensity of the $H_{0-2}O^+$ peak group (*m/z* 16–18) upon NR versus CAD. The most probable reason is partial dissociation of $LiOH_2$ to $Li+H_2O$, followed by a more efficient reionization of H_2O (than Li) due to its higher kinetic energy and reionization cross section [24]. Additionally, the surviving $LiOH_2$ molecules may preferentially reionize to H_nO^+ (versus Li^+) because the charge distribution in $LiOH_2$ provides a partial positive charge to the OH_2 ligand [1].

The NR spectrum of Li^+NH_3 (*m/z* 24) is shown in Fig. 4 and contains a sizable recovery peak. The contamination of this peak by $^6Li^+OH_2$ is very small based on the abundance of $H_2O^{+\cdot}$ (*m/z* 18) relative to the recovery peaks in Figs. 3 and 4 (~1%). Hence, most *m/z* 24 (99%) in the NR spectrum of Li^+NH_3 represents surviving $LiNH_3$ and this complex must also be a stable species in the rarified gas phase, in agreement with the numerous, earlier theoretical predictions [1,2,5]. NR of Li^+NH_3 produces a larger proportion of NH_n^+ (*m/z* 14–17) as compared to CAD. This observation can be accounted for by the same

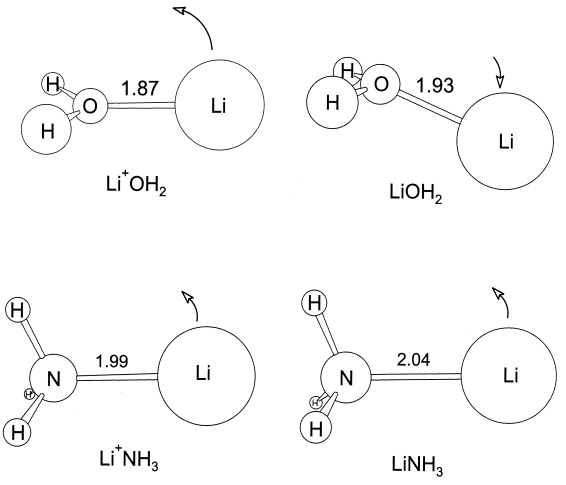

Fig. 5. Computationally predicted structures of Li^+OH_2, $LiOH_2$, Li^+NH_3, and $LiNH_3$ [MP2/6-311++G(*d*,*p*) level of theory].

rationales given for the increased production of H_nO^+ upon NR versus CAD of Li^+OH_2 (vide supra).

3.3. Ab initio calculations

Charge exchange neutralization of fast-moving (kiloelectron volts) cations takes place within femtoseconds and, hence, is a vertical process producing the incipient neutrals in the geometries of the respective ions. For a better understanding of the NRMS results, the structures and energies of the $Li^+OH_2/LiOH_2$ and $Li^+NH_3/LiNH_3$ pairs were assessed by ab initio calculations. The most stable structures found are depicted in Fig. 5; the Li–N and Li–O bond lengths in the neutral complexes are longer than those in the corresponding ion complexes. Except for their difference in Li–N bond lengths, the geometries of Li^+NH_3 and $LiNH_3$ are very similar. In contrast, the optimized geometries of $LiOH_2$ and Li^+OH_2 differ more; in the neutral complex, Li binds to one of the sp^3 lone electron pairs of O, whereas in the ionic complex, Li^+ is attached to a sp^2-hybridized O atom. As a result, Li^+OH_2 has a planar structure, but $LiOH_2$ is nonplanar, with Li bent off the H_2O plane by 40.1°. These trends suggest that the transition between Li^+NH_3 and $LiNH_3$ has a more favorable Franck-Condon factor than that between Li^+OH_2 and $LiOH_2$. Figs. 6 and 7

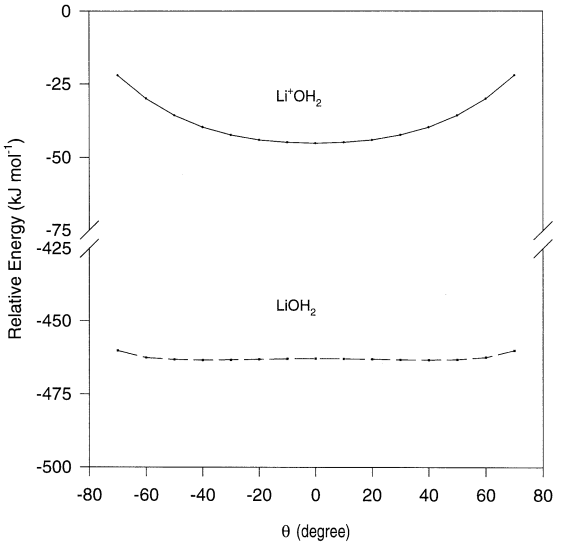

Fig. 6. Potential energy surfaces of Li^+OH_2 and $LiOH_2$ along the Li out-of-plane bending coordinate θ. The relative energies at each point were calculated at the MP2/6-311++G(*d*,*p*) level of theory on partially optimized structures.

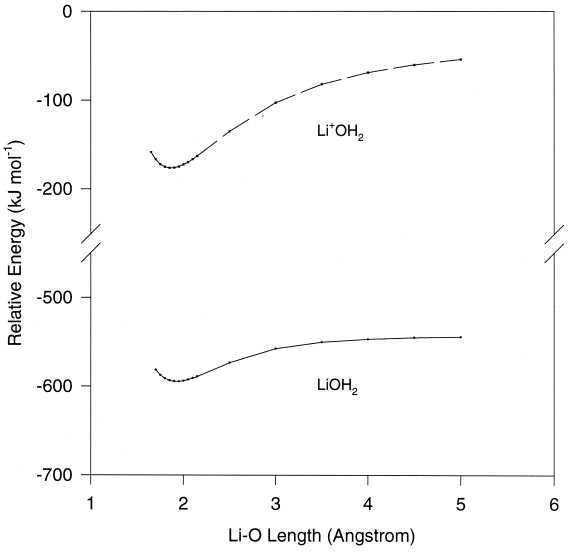

Fig. 8. Potential energy surfaces of Li^+OH_2 and $LiOH_2$ along the Li–O coordinate. The relative energies at each point were calculated at the MP2/6-311++G(*d*,*p*) level of theory on partially optimized structures.

show the potential energy surfaces of the $LiOH_2$/Li^+OH_2 and $LiNH_3$/Li^+NH_3 systems, respectively, as a function of the bending angle θ (defined in Fig. 5).

For $LiOH_2$, the energy diagram indicates that Li atom can freely bend off the H_2O plane, switching between the two lone electron pairs of O; the

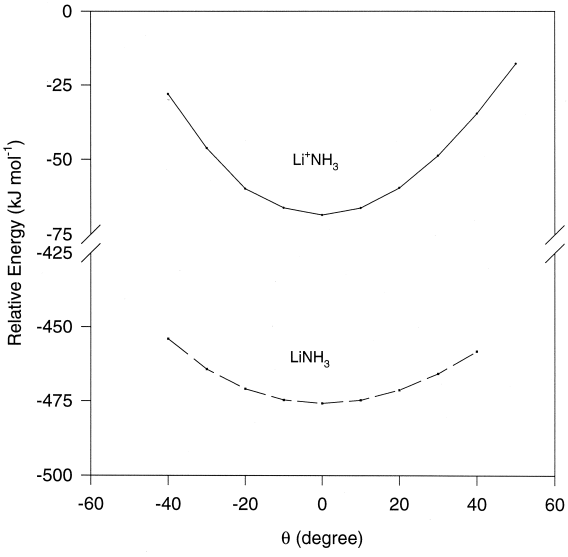

Fig. 7. Potential energy surfaces of Li^+NH_3 and $LiNH_3$ along the Li bending coordinate θ. The relative energies at each point were calculated at the MP2/6-311++G(*d*,*p*) level of theory on partially optimized structures.

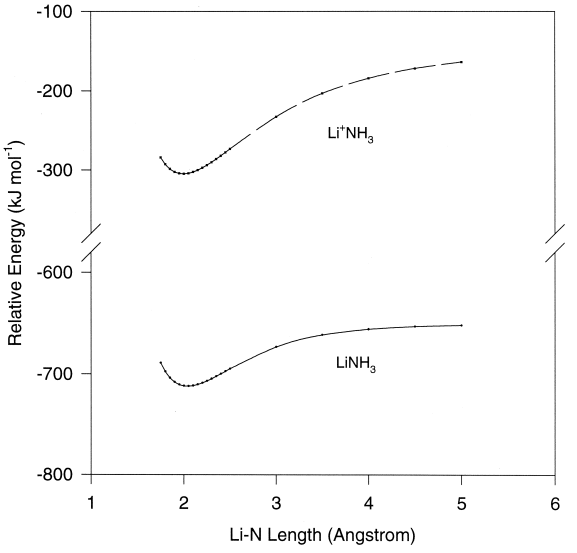

Fig. 9. Potential energy surfaces of Li^+NH_3 and $LiNH_3$ along the Li–N coordinate. The relative energies at each point were calculated at the MP2/6-311++G(*d*,*p*) level of theory on partially optimized structures.

Table 1
Calculated energy data for the LiM/Li^+M complexes (M = OH_2, NH_3)

	EA_v[a] (eV)	IE[a] (eV)	D^+ Li^+–M (kJ mol^{-1})		D^0 Li–M (kJ mol^{-1})		$D^{*,b}$ [Li–M]* (kJ mol^{-1})
			a	Lit.	a	Lit.	a
$LiOH_2$		4.39			51	42[c]	50
$LiNH_3$		4.23			62		61
Li^+OH_2	4.32		148	137–172,[d] 137[e]			
Li^+NH_3	4.21		170				

[a] This study, MP2/6-311++G(*d,p*)//MP2/6-311++G(*d,p*) level.
[b] Dissociation energy of Li–M in the geometry of L^+–M.
[c] Computational value from [35], MP2/6-31++G(*d,p*)//HF6-31++G(*d,p*) level.
[d] Range of MP2 computational values obtained with different basis sets, from [36] (149 kJ mol^{-1} with the basis of our study).
[e] Experimental value from [37].

barrier of the latter process is only 0.04 kJ mol^{-1}. In contrast, Li atom or Li^+ ions are more rigid at their positions in the other three complexes, the resistance in θ deformation increasing in the order $Li^+OH_2 < Li^+NH_3 \approx LiNH_3$.

Because the neutral complexes are mostly stabilized by Li–O or Li–N bonds, potential energy surfaces along the Li–O or Li–N coordinates have also been constructed for the $Li^+OH_2/LiOH_2$ and $Li^+NH_3/LiNH_3$ pairs and are shown in Figs. 8 and 9, respectively. The two sets of potential energy surfaces are very comparable. Table 1 summarizes important energy data that can be extracted from these diagrams, including the vertical electron affinities of Li^+OH_2 and Li^+NH_3 (EA_v), the adiabatic ionization energies of $LiOH_2$ and $LiNH_3$ (IE), the bond energies of the ionic complexes (D^+), and the bond energies of the neutral complexes both in their equilibrium geometries (D^0) as well as in the geometries of the corresponding cations (D^*); recent literature values are also included. The data in Table 1 reveal that $LiOH_2/Li^+OH_2$ and $LiNH_3/Li^+NH_3$ have similar thermochemical properties, with Li^+NH_3 recovery upon NR being slightly favored by thermochemistry and Franck-Condon overlap.

4. Conclusions

The neutral complexes $LiOH_2$ and $LiNH_3$ have been synthesized and characterized in the gas phase by neutralization–reionization mass spectrometry. In addition, ab initio theory was applied to assess the stability of the complexes and the gas-phase redox properties of the pairs $LiOH_2/Li^+OH_2$ and $LiNH_3/LiNH_3^+$. The ionization energies of $LiOH_2$ and $LiNH_3$ are very similar. On the other hand, the NH_3 complexes have slightly higher binding energies both in the neutral and cationic states. A major difference between the most stable structures of $LiOH_2$ and $LiNH_3$ is a high mobility of Li atoms in $LiOH_2$, where it can freely bend off the H_2O plane within a range of ~90°, but a high rigidity of Li atom in $LiNH_3$. This gives a better Franck-Condon overlap to transitions between Li^+NH_3 and $LiNH_3$ than to transitions between Li^+OH_2 and $LiOH_2$. When subjected to NR, the ammonia complexes benefit from a more favorable Franck-Condon factor and somewhat higher thermodynamic stabilities; as a result, less dissociation takes place, which is reflected by the higher recovery yield of neutralized–reionized Li^+NH_3.

Acknowledgement

This work was generously supported by the National Science Foundation (CHE-9725003).

References

[1] M. Trenary, H.F. Schaefer III, P. Kollman, J. Am. Chem. Soc. 99 (1977) 3885.
[2] V.A. Nicely, J.L. Dye, J. Chem. Phys. 52 (1970) 4795.

[3] M. Trenary, H. F. Schaefer III, P. A. Kollman, J. Chem. Phys. 68 (1978) 4047.
[4] L.A. Curtiss, D.J. Frurip, Chem. Phys. Lett. 75 (1980) 69.
[5] J. Bentley, I. Carmichael, J. Phys. Chem. 85 (1981) 3821.
[6] J. Bentley, J. Am. Chem. Soc. 104 (1982) 2754.
[7] J.Q. Broughton, P.S. Bagus, J. Chem. Phys. 77 (1982) 3627.
[8] L.A. Curtiss, J.A. Pople, J. Chem. Phys. 82 (1985) 4230.
[9] L.A. Curtiss, E. Kraka, J. Gauss, D. Cremer, J. Phys. Chem. 91 (1987) 1080.
[10] E.-U. Würthwein, P.v.R. Schleyer, J.A. Pople, J. Am. Chem. Soc. 106 (1984) 6973.
[11] Y.-W. Hsiao, K.-M. Chang, T.-M. Su, Chem. Phys. 162 (1992) 335.
[12] H. Yang, Y.-H. Liau, T.-M. Su, J. Phys. Chem. 99 (1995) 177.
[13] R.H. Hauge, P.F. Meier, J.L. Margrave, Ber. Bunsenges. Phys. Chem. 82 (1978) 102.
[14] J.E. Douglas, P.A. Kollman, J. Am. Chem. Soc. 102 (1980) 4295.
[15] P.F. Meier, R.H. Hauge, J.L. Margrave, J. Am. Chem. Soc. 100 (1978) 2108.
[16] Z.H. Kafafi, R.G.S. Pong, J.S. Shirk, J. Mol. Struct. 222 (1990) 245.
[17] A. Loutellier, L. Manceron, J.P. Perchard, Chem. Phys. 146 (1990) 179.
[18] C.P. Schulz, R. Haugstätter, H.-U. Tittes, I.V. Hertel, Phys. Rev. Lett. 57 (1986) 1703.
[19] C.P. Schulz, R. Haugstätter, H.-U. Tittes, I.V. Hertel, Z. Phys. D: At. Mol. Clusters 10 (1988) 279.
[20] T.-C. Kuan, R.-C. Jiang, T.-M. Su, J. Chem. Phys. 92 (1990) 2553.
[21] I.V. Hertel, C. Hüglin, C. Nitsch, C.P. Schulz, Phys. Rev. Lett. 67 (1991) 1767.
[22] R. Takasu, K. Hashimoto, K. Fuke, J. Phys. Lett. 258 (1996) 94.
[23] R. Takasu, F. Misaizu, K. Hashimoto, K. Fuke, J. Phys. Chem. A 101 (1997) 3078.
[24] C. Wesdemiotis, F.W. McLafferty, Chem. Rev. 87 (1987) 485.
[25] J.K. Terlouw, H. Schwarz, Angew. Chem. Int. Ed. Engl. 26 (1987) 805.
[26] J.L. Holmes, Mass Spectrom. Rev. 8 (1989) 513.
[27] N. Goldberg, H. Schwarz, Acc. Chem. Res. 27 (1994) 347.
[28] D.V. Zagorevskii, J.L. Holmes, Mass Spectrom. Rev. 13 (1994) 133; 18 (1999) 87.
[29] M.J. Polce, C. Wesdemiotis, Int. J. Mass Spectrom. 182/183 (1999) 45.
[30] J. Wu, C. Wesdemiotis, Chem. Phys. Lett. 303 (1999) 243.
[31] M.J. Polce, M.M. Cordero, C. Wesdemiotis, P.A. Bott, Int. J. Mass Spectrom. Ion Processes 113 (1992) 35.
[32] M.J. Frisch, G.W. Trucks, H.B. Schlegel, P.M.W. Gill, B.G. Johnson, M.A. Robb, J.R. Cheeseman, T.A. Keith, G. . Petersson, J.A. Montgomery, K. Raghavachari, M.A. Al-Laham, V.G. Zakrzewski, J.V. Ortiz, J.B. Foresman, J. Cioslowski, B.B. Stefanov, A. Nanayakkara, M. Challocombe, C.Y. Peng, P.Y. Ayala, W. Chen, M.W. Wong, J.L. Andres, E.S. Replogle, R. Gomperts, R.L. Martin, D.J. Fox, J.S. Binkley, D.J. Defrees, J. Baker, J.J.P. Stewart, M. Head-Gordon, C. Gonzalez, J.A. Pople, GAUSSIAN 94, Gaussian, Inc., Pittsburgh, PA, 1995.
[33] CHEM-3D, CambridgeSoft Corporation, Cambridge, MA.
[34] K.L. Busch, G.L. Glish, S.A. McLuckey, Mass Spectrometry/Mass Spectrometry, VCH, New York, 1988.
[35] K. Hashimoto, T. Kamimoto, J. Am. Chem. Soc. 120 (1998) 3560.
[36] D. Feller, E.D. Glendening, R.A. Kendall, K.A. Peterson, J. Chem. Phys. 100 (1994) 4981.
[37] M.T. Rodgers, P.B. Armentrout, J. Phys. Chem. A 101 (1997) 1238.